



Synthesis and structures of amido-functionalized N-heterocyclic nickel(II) carbene complexes



Sheng-Zhi Lu^a, Hsueh-Hui Yang^b, Wei-Ju Chang^a, Hsin-Hsueh Hsueh^a, Yong-Chieh Lin^a, Fu-Chen Liu^{a,*}, Ivan J.B. Lin^a, Gene-Hsiang Lee^c

^a Department of Chemistry, National Dong Hwa University, Hualien 974, Taiwan, ROC

^b Department of Medical Research, Hualien Tzu Chi Hospital, Buddhist Tzu Chi Foundation, Hualien, 970, Taiwan, ROC

^c Department of Chemistry, National Taiwan University, Taipei 106, Taiwan, ROC

ARTICLE INFO

Article history:

Received 14 July 2020

Revised 17 September 2020

Accepted 21 September 2020

ABSTRACT

A series of bis-bidentate nickel(II) complexes $[\text{Ni}(\text{R-bimy-CH}_2\text{CONH})_2]$ (bimyH = benzimidazole; R = Me (**3**), Et (**4**), Ph (**5**)) bearing amido-functionalized N-heterocyclic carbene ligands, and pincer-type nickel(II) complexes $[\text{Ni}(\text{Py-bimy-CH}_2\text{CONH})\text{X}]$ (X = Cl (**6**), Br (**7**))) bearing an amido- and pyridyl-functionalized N-heterocyclic carbene ligand were prepared. These complexes were characterized by NMR (1D and 2D) and single-crystal X-ray diffraction. Complexes **3–5** possess *cis* configuration, and the carbene ligands bound to the nickel atom through C2 carbon and NH nitrogen in a bis-bidentate coordination mode. In complexes **6** and **7**, the pyridyl substituent was also N-bound to the nickel metal center resulting in a pincer-type coordination mode. As observed from the proton NMR spectra, the six-membered chelate rings in complexes **3–5** rendered the protons of the methylene moieties diastereotopic, and the *cis* configuration made the free rotation of the ethyl substituent in **4** and the phenyl substituent in **5** hampered by the adjacent substituent. The catalytic activity of these nickel complexes in Kumada cross-coupling of phenylmagnesium bromide with aryl chlorides was also investigated. The results indicated that pincer-type complexes **6** and **7** displayed excellent to moderate catalytic activity depending on the aryl chloride used.

© 2020 Elsevier B.V. All rights reserved.

1. Introduction

Since the isolation of a stable N-heterocyclic carbene (NHC) by Arduengo et al. in 1991 [1], the study of transition metal complexes with NHC ligands has become one of the most exciting research topics in organometallic chemistry. Numerous transition metal-NHC complexes have been prepared and studied in the past decades. The main reason for such a rich chemistry is the ability to tune the electronic and steric properties of the NHC ligands by modifying substituents [2]. These properties make NHC complexes catalytically active in various reactions [3]. For example, palladium NHC complexes have been used as pre-catalysts in numerous C-C cross-coupling reactions [4], which are of great importance in organic chemistry. Although nickel NHC complexes have not been studied as extensively as their palladium analogues, a significant amount of work has been published recently [5] on such diverse catalytic applications as Suzuki-Miyaura and Kumada cross-coupling [6,7], olefin polymerization [8], C-H bond activation [9], and reduction of carbon dioxide [10].

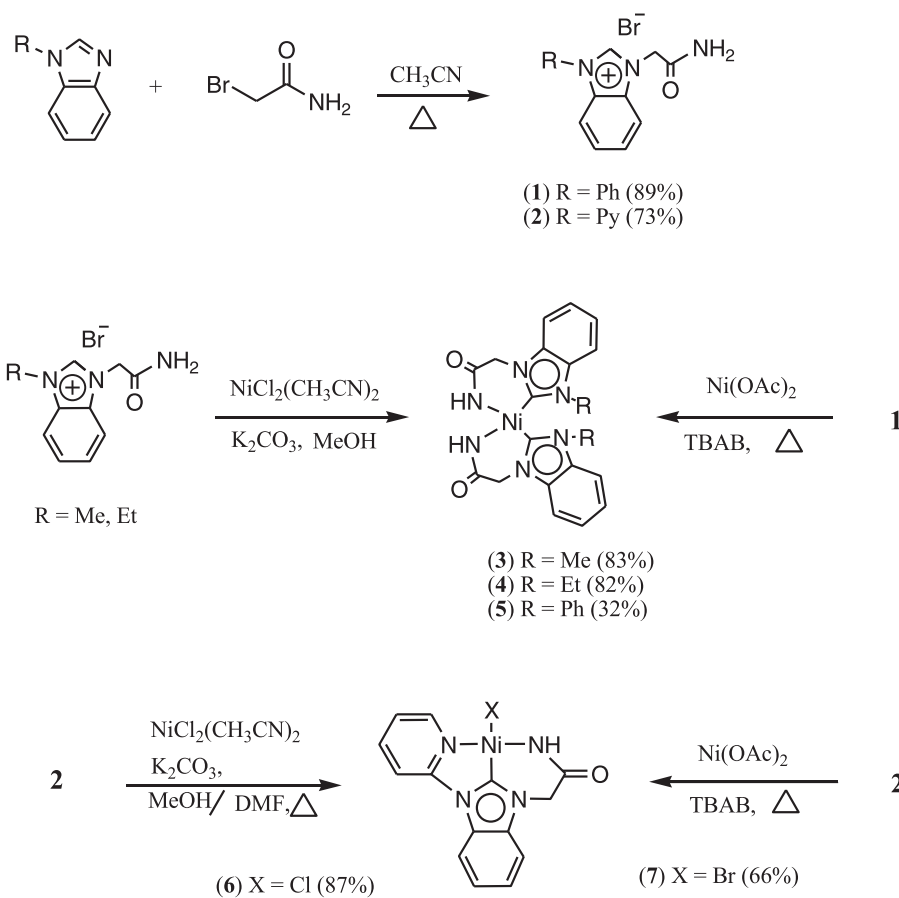
Recently, N-heterocyclic carbene complexes containing donor atoms (e.g. C, N, O, S, or P) have attracted considerable attention, as these complexes showed enhanced activity in many catalytic reactions [11]. As continuation of our studies of transition metal complexes with amido-functionalized NHC carbene ligands [12], here we report the preparation and characterization of several amido-functionalized NHC bis-bidentate and pincer-type nickel(II) carbene complexes as well as the catalytic activity of these complexes in Kumada cross-coupling of phenylmagnesium bromide with aryl chlorides.

2. Results and discussion

2.1. Amido-functionalized NHC ligand precursors **1** and **2**

The amido-functionalized NHC ligand precursors 1-acetamido-3-phenylbenzimidazolium bromide (**1**), and 1-acetamido-3-(2-pyridyl)benzimidazolium bromide (**2**) (Scheme 1), were prepared from the reactions of 2-bromoacetamide with 1-phenylbenzimidazole [13] and 1-(2-pyridyl)benzimidazole [14], respectively, in refluxing acetonitrile. Both compounds are soluble in water, MeOH, DMF, and DMSO; and slightly soluble in acetone,

* Corresponding author.



Scheme 1. Synthetic route to prepare the NHC salts **1-2** and the NHC nickel (II) complexes **3-7**.

THF, and acetonitrile. In the proton NMR spectra of **1** and **2** (DMSO-d₆), the diagnostic acidic benzimidazolium NCHN proton appears at 10.39 and 10.60 ppm, respectively. These chemical shifts are about 2.0 ppm downfield relative to the corresponding signals of the benzimidazoles. The ¹J_{CH} coupling constant of the NCHN proton is 222.9 Hz for **1** and 198.2 Hz for **2**. Azolium salts ¹J_{CH} coupling constants have been used to estimate the σ -donor ability of the NHC ligands [15]. The higher the value of the coupling constant is, the poorer the σ -donating property of a NHC ligand would be. This result suggested that the pyridyl group would induce more σ -donating property than the phenyl group. The methylene protons appear at 5.47 ppm in **1** and 5.43 ppm in **2**. The amido protons of **1** (7.75 and 8.15 ppm) and **2** (7.76 and 8.07 ppm) are not equivalent due to a partial double bond character of the C(O)-NH₂ bond [12a], and these chemical shifts are slightly downfield compared with those of 2-bromooacetamide (7.25 and 7.62 ppm). The NCHN and carbonyl carbon signals appear at 144.02 and 166.66 ppm in **1**, and 147.56 and 166.52 ppm in **2**, respectively, in the ¹³C NMR spectra.

2.2. Nickel(II) bis-carbene complexes **3-5**

Treatment of NiCl₂(CH₃CN)₂ and K₂CO₃ with the amido-functionalized ligand precursor 1-acetamido-3-methylbenzimidazolium bromide [12a] or 1-acetamido-3-ethylbenzimidazolium bromide [12b] in hot methanol yielded the nickel(II) bis-carbene complex [Ni(R-bimy-CH₂CONH)₂] (R = Me (**3**), Et (**4**)) shown in Scheme 1. When the same method was applied to prepare the nickel(II) bis-carbene complexes [Ni(Ph-bimy-CH₂CONH)₂] (**5**), it failed due to the formation and decomposition

of complex **5** occurring simultaneously in the reaction. Complex **5** could not be separated from the unidentified by-products. Eventually, complex **5** was prepared through an alternative method from the reaction of Ni(OAc)₂ with **1** in hot [Bu₄N]Br (TBAB), which is known as a basic metal precursor method [16]. Complexes **3-5** are air-stable solids and very soluble in DMSO, DMF, and MeOH; but only slightly soluble in THF, acetonitrile, and acetone. Attempts to prepare the corresponding mono-carbene complexes failed. Only the bis-carbene complexes were observed and isolated from the reactions when the ratio of the metal precursor to the corresponding benzimidazolium salt was 1:1.

The formation of the bis-bidentate nickel complexes is suggested by the absence of the carbenic proton and one of the amido proton resonances in their ¹H NMR spectra. The remaining amido proton appeared at 4.49 ppm in **3**, 4.52 ppm in **4**, and 4.62 ppm in **5**. These chemical shifts are about 3.5 ppm upfield relative to the signals of the NH₂ protons of the parent benzimidazolium salts, and consistent with the anionic nature of the amido ligand. Coordination of the amido nitrogen and the carbene carbon atoms to nickel produces a six-membered chelate ring, which renders the protons of the methylene groups diastereotopic. Two well-resolved doublets (4.75 and 5.19 ppm in **3**, 4.78 and 5.09 ppm in **4**, and 4.42 and 4.50 ppm in **5**) with a two-bond geminal coupling (²J_{HH}) of 16 Hz were observed in their proton NMR spectra. The signals of these methylene protons were found to be fluxional. Variable-temperature proton NMR spectra of complex **4** are shown in Fig. 1 to describe this behavior. At room temperature, two well-resolved doublets at 4.78 and 5.09 ppm corresponding to the diastereotopic protons of the two methylene groups were observed. As the temperature increased, these two signals broadened and coalesced at

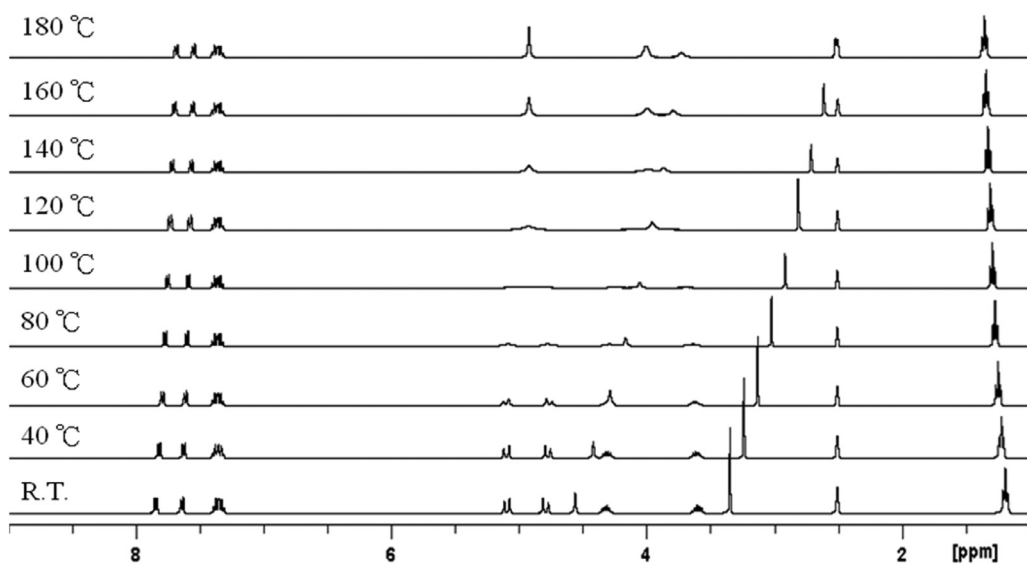


Fig. 1. Variable temperature ^1H NMR spectra of **4** in $\text{DMSO}-d_6$

about 100 °C, and an average broad signal appeared. As the temperature increased further, this signal sharpened, and at 180 °C it appeared as a sharp singlet at 4.92 ppm. The fluxional behavior of the methylene protons could be caused either by bond cleavage (Ni-N or Ni-C) or fast vibration of the chelate rings at high temperature. However, the cleavage of the Ni-N or Ni-C bond could be energetically unfavorable, and our VT-NMR studies did not produce any evidence to support it. As shown in Fig. 1, the NH proton resonance shifted upfield gradually as the temperature was raised. This result may suggest that the Ni-N bond weakens but the molecule is still intact at the higher temperature. Thus, the fast vibration of the chelate rings is more likely to account for the fluxional behavior.

An additional interesting feature of the proton NMR spectrum of complex **4** shown in Fig. 1 is that two methylene protons of the ethyl groups are inequivalent at 3.59 and 4.31 ppm. As the single crystal X-ray structure determination of complexes **3–5** (see below) has confirmed the *cis* configuration, which results in steric hindrance and restricts the free rotation of the two ethyl substituents in complex **4**. The free rotation of these two ethyl groups can be achieved at high temperature as shown in Fig. 1, where these two signals first broaden and then coalesce at about 120 °C. Finally, at 180 °C an average broad signal appears at 4.00 ppm. The same steric effect was also observed in the proton NMR spectrum of complex **5**, in which the phenyl group appeared as two broad signals at 7.88 and 7.36 ppm at room temperature, and re-appeared as a doublet at 7.86 ppm and a triplet at 7.37 ppm at 80 °C (Fig. S1 in the Supporting Information).

Upon the formation of the nickel carbene complexes, the C2 carbon signal shifted to the general carbonyl resonance region. 2D ^{13}C - ^1H HMBC NMR technique was used to assign the carbonyl and C2 carbon signals unambiguously. For example, in the 2D NMR spectrum of **4** (Fig. S2 in the Supporting Information), the carbon signal which had significant correlation with the amido and methylene protons of the amido substituent was assigned to the carbonyl group, while the carbon signal which has significant correlation with the methylene protons of the ethyl substituent was assigned to the C2 carbon. The C2 and carbonyl carbon chemical shifts appeared at 178.55 and 170.83 ppm in **3**, 178.43 and 170.90 ppm in **4**, and 180.15 and 170.34 ppm in **5**, respectively. These C2 carbon chemical shifts are about 35 ppm down-field relative to the corresponding signals of the benzimidazolium salts.

2.3. Pincer-type nickel(II) carbene complexes **6** and **7**

Similar to the syntheses of **3** and **4**, we carried out the reaction of $\text{NiCl}_2(\text{CH}_3\text{CN})_2$ with 1-acetamido-3-(2-pyridyl)benzimidazolium bromide (**2**) and K_2CO_3 in refluxing methanol solution. During the reaction, we observed the formation of pincer complex $[\text{Ni}(\text{Py-bimy-CH}_2\text{CONH})\text{Cl}]$ (**6**). However, it had decomposed before the reaction was complete. After several attempts, we found that decomposition was induced by K_2CO_3 , a relative strong base. Thus, we replaced potassium carbonate with sodium acetate, which is a weaker base, and carried out the reaction in MeOH-DMF (1:3) at 120 °C. Under these conditions complex **6** was isolated in 87% yield. It is interesting to note that the strong base potassium carbonate is the only base that has been used to remove the amido proton of the amido-functionalized carbene ligand precursors [17], and the use of a weaker base such as sodium acetate has never been reported before. To increase the solubility and compare the catalytic activity, we also prepared the corresponding bromo analog $[\text{Ni}(\text{Py-bimy-CH}_2\text{CONH})\text{Br}]$ (**7**) from the reaction of $\text{Ni}(\text{OAc})_2$ with **2** in TBAB. Complexes **6** and **7** are air-stable and slightly soluble in highly polar solvents such as DMSO, DMF, and H_2O . The solubility of complex **7** is only slightly better than that of complex **6**.

In the proton NMR spectra of **6** and **7**, the remaining amido proton appeared at 3.73 and 4.15 ppm, respectively. These chemical shifts are slightly upfield compared to those found in complexes **3–5**. Coordination of the amido nitrogen atom also produced a six-membered chelate ring in both cases; however, the symmetric planar structure in solution made the two methylene protons steric equivalent and only one proton signal (4.84 ppm in **6** and 4.88 ppm in **7**) was observed. Due to their low solubility, the ^{13}C NMR spectra of these complexes have not been acquired.

2.4. Molecular structures of **3–7**

Crystals of **3**, **4**, and **5** suitable for X-ray diffraction analyses were obtained as described in the experimental section; all structures were found to contain solvent molecules in their unit cell. Figs. 2–4 show the molecular structures of **3–5** with selected bond distances and bond angles listed in the captions. Although the unit cell of **4** contains two crystallographically different molecules, only one molecule is displayed due to the difference is insignificant. In

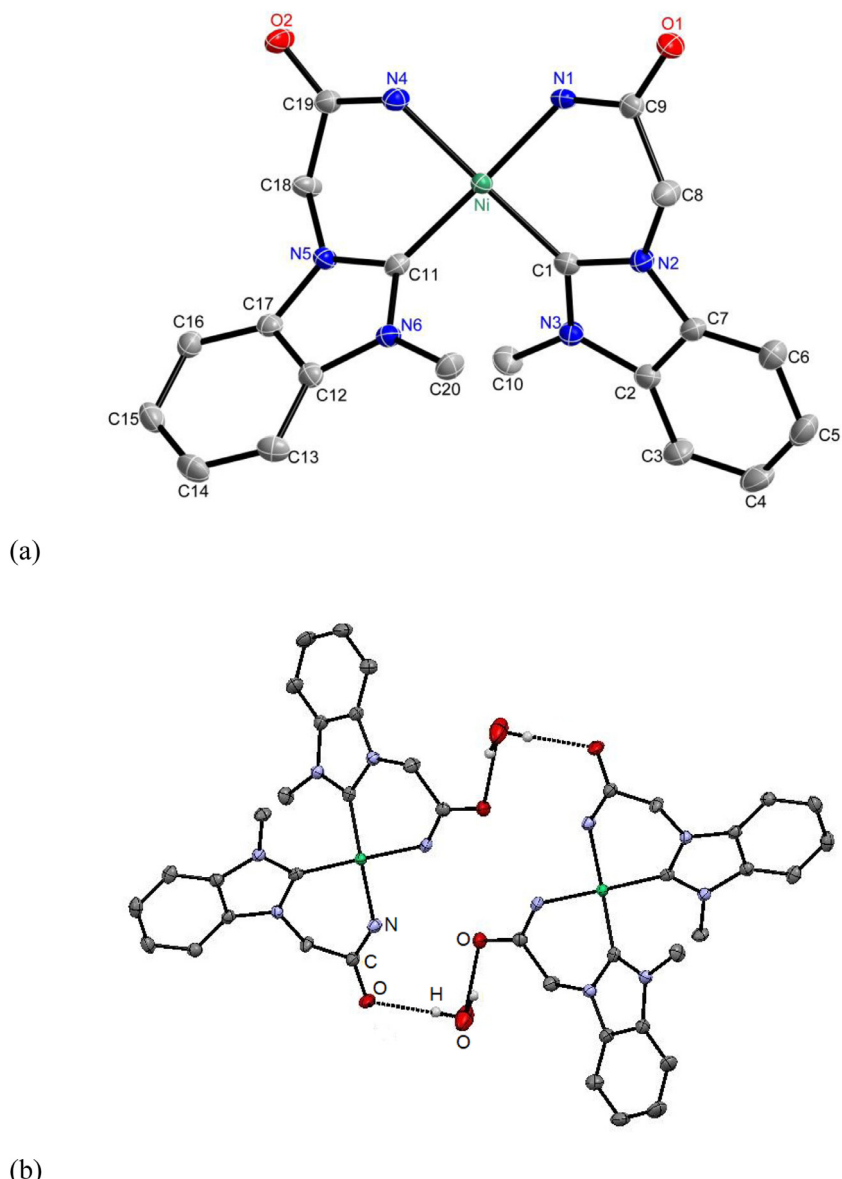


Fig. 2. (a) Thermal ellipsoid plot of **3** at 50% probability level. Hydrogen atoms and solvent molecules are omitted for clarity. (b) Extended structure of **3**. Selected bond lengths (\AA) and angles ($^\circ$): Ni-C(11), 1.852(3); Ni-C(1), 1.854(3); Ni-N(1), 1.891(2); Ni-N(4), 1.897(2); N(1)-C(9), 1.307(4); N(4)-C(19), 1.316(4); C(11)-Ni-C(1), 92.83(12); C(11)-Ni-N(1), 168.46(11); C(1)-Ni-N(1), 89.95(11); C(11)-Ni-N(4), 88.39(11); C(1)-Ni-N(4), 170.12(11); N(1)-Ni-N(4), 90.78(10); N(2)-C(1)-N(3), 105.7(2); N(5)-C(11)-N(6), 106.1(2).

each complex, the nickel atom is coordinated by two bidentate carbene ligands in *cis* configuration. The dihedral angles between the two planes defined by the nickel atom and the coordinating atoms in each bidentate ligand are 15.20° in **3**, 12.69 and 15.65° in **4**, and 13.31° in **5**. The *trans*-angles are 168.46(11) and 170.12(11)° in **3**, 169.89(8) and 171.46(8)° (one molecule), and 167.77(8) and 169.62(8)° (the other molecule) in **4**, and 168.96(9) and 171.97(9)° in **5**, reflecting a slightly distorted square planar geometry for each complex. The Ni-C bond distances (1.852(3)-1.8711(17) \AA) found in complexes **3-5** are comparable to other nickel(II) *cis* bis(carbene) complexes [17a-d,18]. The Ni-N bonds (1.8874(19)-1.9018(15) \AA) in complexes **3-5** are longer than the sum of the covalent radii of nickel and nitrogen atoms (Ni-N = 1.854 \AA) [19], but they are shorter than those reported for the nickel(II) *cis* bis(carbene) complexes with other amido-functionalized NHC ligands [17a-d] due to the less stringent steric requirement imposed by the NH protons. The N-C(O) bond distances (1.304(3)-1.322(3) \AA) in these complexes are shorter than the sum of the individual single bond

covalent radii of C (0.772 \AA) and N (0.70 \AA) [20], reflecting the partial double bond character of the amido substituent. The six-membered chelate rings adopt a boat conformation in all cases.

In addition, extended structures through hydrogen bonding interactions have been found in all cases. In compound **3**, two molecules of **3** are connected to two water molecules through the C=O groups to form a macrocycle. The O...O distances are 2.747 and 2.846 \AA , respectively. In compound **4**, a C=O group and an NH group in one molecule are hydrogen-bonded to their neighboring molecule to form a dimeric structure. The O...N distances are 3.044 and 3.060 \AA , respectively. In complex **5**, both solvent molecules (CH_3OH and water) are all involved in the hydrogen bonding interaction, and the O...O distances in the range of 2.703-2.843 \AA are observed. The intermolecular hydrogen bonding interaction between the C=O group of **5** and the water molecules produces a 1D polymeric structure.

Crystals of **6** and **7** suitable for single crystal X-ray diffraction analyses were obtained from a DMSO/ether/EA mixed solvent sys-

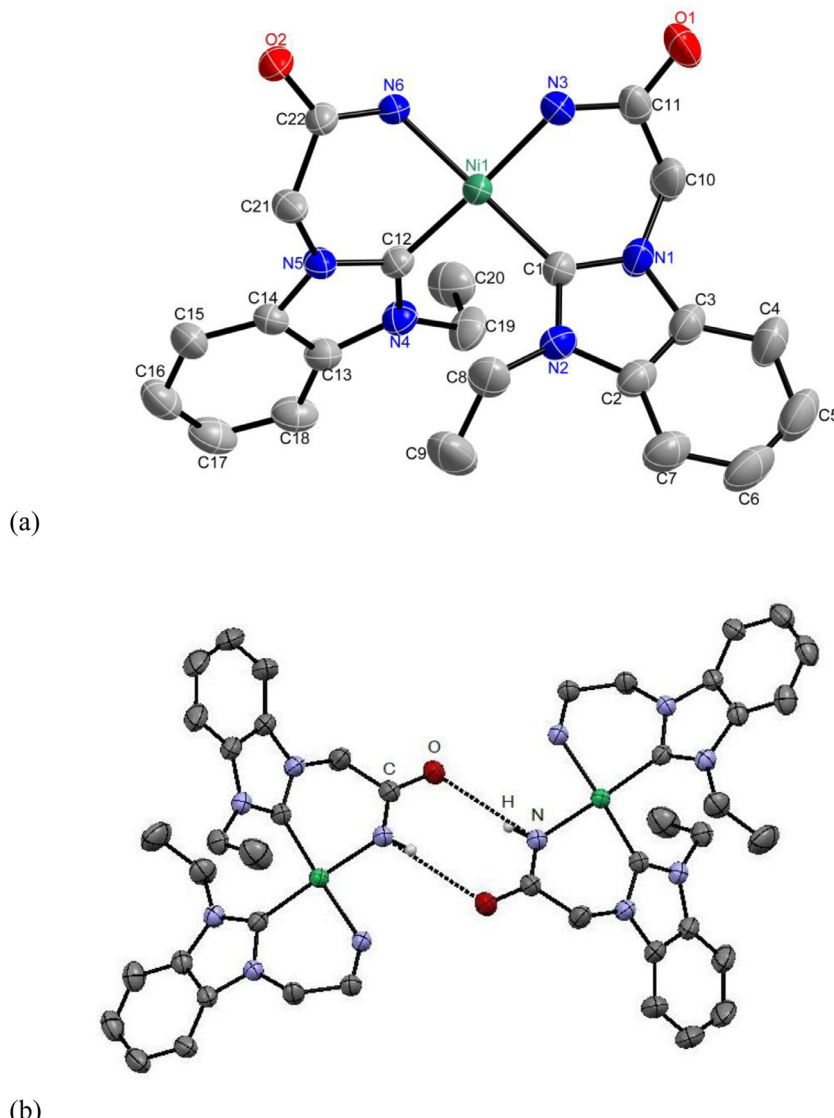


Fig. 3. (a) Thermal ellipsoid plot of **4** at 50% probability level. Hydrogen atoms and solvent molecules are omitted for clarity. (b) Extended structure of **4**. Selected bond lengths (\AA) and angles ($^\circ$): Ni(1)-C(12), 1.8613(18); Ni(1)-C(1), 1.8677(18); Ni(1)-N(3), 1.8904(17); Ni(1)-N(6), 1.8907(15); C(34)-Ni(2), 1.8711(17); C(23)-Ni(2), 1.8640(18); N(9)-Ni(2), 1.8934(15); Ni(2)-N(12), 1.9018(15); N(3)-C(11), 1.322(3); N(6)-C(22), 1.310(2); N(9)-C(33), 1.311(2); N(12)-C(44), 1.313(2); C(12)-Ni(1)-C(1), 95.02(8); C(12)-Ni(1)-N(3), 171.46(8); C(1)-Ni(1)-N(3), 88.42(8); C(12)-Ni(1)-N(6), 87.92(7); C(1)-Ni(1)-N(6), 169.89(8); N(3)-Ni(1)-N(6), 90.03(7); N(1)-C(1)-N(2), 105.97(16); N(5)-C(12)-N(4), 106.01(15); N(11)-C(34)-N(10), 106.02(15); N(8)-C(23)-N(7), 106.00(15); C(23)-Ni(2)-C(34), 95.71(7); C(23)-Ni(2)-N(9), 88.41(7); C(23)-Ni(2)-N(9), 169.62(8); C(34)-Ni(2)-N(12), 167.77(8); C(34)-Ni(2)-N(12), 88.45(7); N(9)-Ni(2)-N(12), 89.47(7).

tem. Complexes **6** and **7** are isostructural, and except for the Ni-X (X = Cl, Br) bond distance, both complexes have similar bond distances and angles. Thus, only the molecular structure of **6** is shown in Fig. 5, and the selected bond distances and bond angles are listed in the captions. The molecular structure of **7** is shown in Fig. S3 of the supporting information. In both compounds, the nickel atom is surrounded by a carbene ligand and a halide ligand. The carbene ligand coordinates to a nickel atom through a carbene carbon and two nitrogen atoms, one from the pyridyl substituent and the other from the amido group, to form a tridentate pincer complex, in which the carbene carbon is *trans* to a halide ligand. The nickel atom is almost coplanar with the plane defined by the four coordinated atoms, and the distance above the defined plane is 0.039 \AA in **6** and 0.041 \AA in **7**. The C-Ni-X (X = Cl or Br) bond angle is linear in the structures of both complexes; it is 177.73(11) $^\circ$ in **6** and 177.4(3) $^\circ$ in **7**. The N-Ni-N bond angle is 170.72(12) $^\circ$ in **6** and 170.1(3) $^\circ$ in **7**. The Ni-C bond distance is 1.790(3) \AA in **6** and 1.799(9) \AA in **7**; both are slightly shorter than those found in other

pincer-type nickel complexes [21]. The Ni-N_{amido} bonds (1.840(3) \AA in **6** and 1.838(7) \AA in **7**) in both complexes are shorter than those found in complexes **3-5**, due to a weak trans influence of the pyridyl group in both complexes. The N-C(O) bond distance is 1.325(4) \AA in **6** and 1.328(12) \AA in **7**, which is slightly longer than those found in complexes **3-5**. The Ni-N_{py} bond distance is 1.932(3) \AA in **6** and 1.933(8) \AA in **7**, which is within the range observed in other nickel complexes containing Ni-N_{py} bond [21]. The Ni-Cl bond distance is 2.2117(10) \AA in **6**, and the Ni-Br bond distance is 2.3520(15) \AA in **7**, these Ni-X (X = Br, Cl) bond distances are comparable to other nickel complexes containing the Ni-X (X = Cl, Br) bonds [21,22]. No extended hydrogen bonding interaction was found in either structure.

2.5. Catalytic studies

The nickel carbene complexes are well-known catalysts for Kumada cross-coupling reaction of organic halides with Grignard

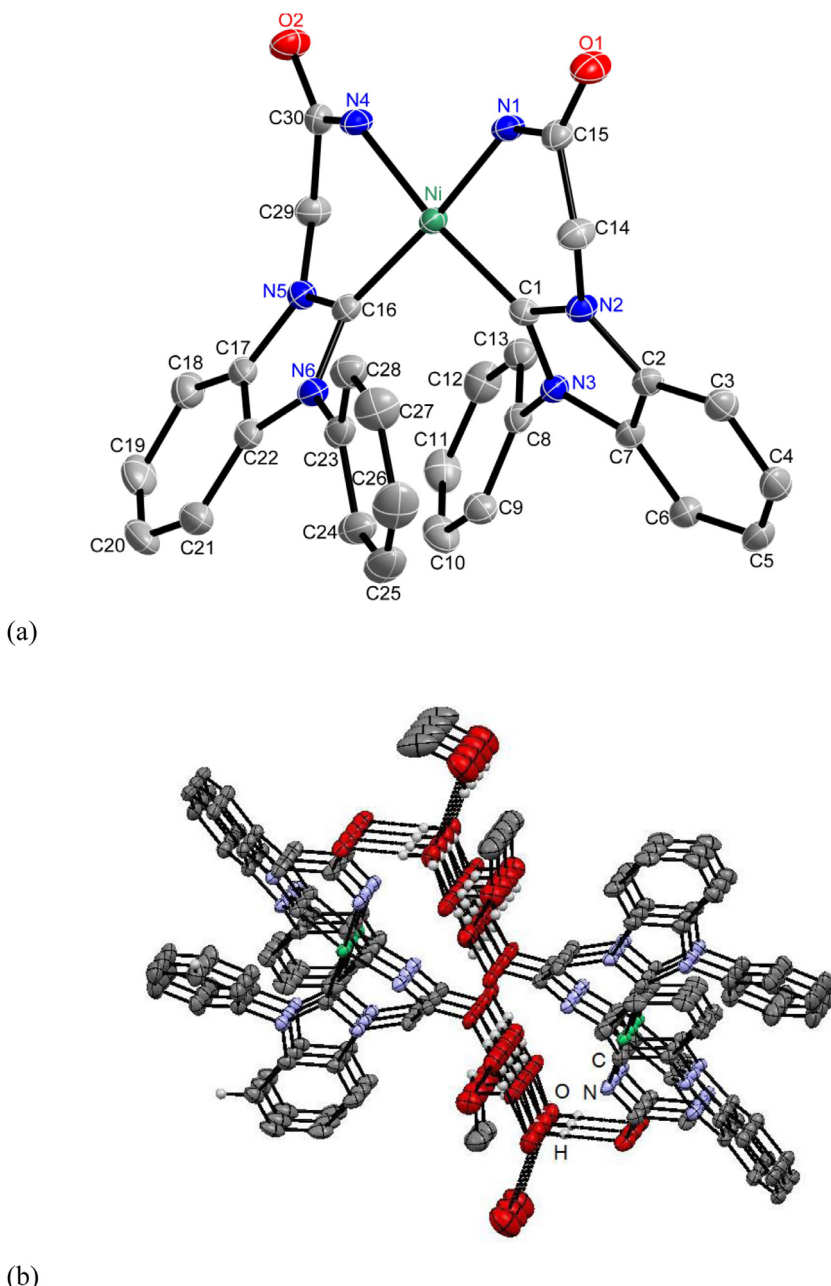


Fig. 4. (a) Thermal ellipsoid plot of **5** at 50% probability level. Hydrogen atoms and solvent molecules are omitted for clarity. (b) Extended structure of **5**. Selected bond lengths (\AA) and angles ($^\circ$): Ni-C(16), 1.859(2); Ni-C(1), 1.859(2); Ni-N(1), 1.8874(19); Ni-N(4), 1.8926(19); N(1)-C(15), 1.310(3); N(4)-C(30), 1.304(3); C(16)-Ni-C(1), 94.31(9); C(16)-Ni-N(1), 171.97(9); C(1)-Ni-N(1), 89.23(9); C(16)-Ni-N(4), 88.57(9); C(1)-Ni-N(4), 168.96(9); N(1)-Ni-N(4), 89.31(8); N(2)-C(1)-N(3), 105.63(18); N(5)-C(16)-N(6), 105.93(18).

reagents [23]. In this study, the catalytic activities of complexes **3-7** were initially tested in the coupling reactions of phenylmagnesium bromide with chlorobenzene. A typical experiment is described in the experimental section. As shown in Table 1, the alkyl-substituted complexes **3** and **4** were the least active catalysts, achieving only 37% yield after 6 h (entries 1 and 2). The phenyl-substituted complex **5** had a better catalytic activity resulting in 49% yield (entry 3). In comparison, both pincer-type complexes **6** and **7** displayed high catalytic activity as the coupling product was obtained in 94 and 96% yields (entries 4 and 5). The different halide substituent in these two complexes did not have a significant effect on their catalytic activity.

It is interesting to note that complexes **6** and **7** alone are not soluble in THF; however, upon addition of phenylmagnesium

bromide and chlorobenzene, the mixture in THF changed color to orange brown immediately, and a homogeneous solution was formed. The color change indicated reduction of the nickel(II) complex into a more active nickel(0) species [24]. It has been reported that the pincer-type complexes possess excellent catalytic performance in many coupling reactions [25]. During the reaction, the hemilabile pyridyl substituent of these two pincer-type complexes could stabilize the coordinatively unsaturated intermediate, which improves the catalytic properties through the reversible coordination of the hemilabile substituent to the metal center resulting in higher catalytic activity.

As complexes **6** and **7** proved to be effective catalysts for the cross-coupling reaction of phenylmagnesium bromide with chlorobenzene, they were further tested on substituted aryl chlo-

Table 1
Kumada cross-coupling reactions of aryl chloride with PhMgBr.

Entry ^a	Catalyst	R	Yield (%) ^b
1	3	H	37
2	4	H	36
3	5	H	49
4	6	H	94
5	7	H	96
6	6	CN	5
7	7	CN	5
8	6	OMe	55 ^c
9	7	OMe	55 ^c
10	6	Me	51 ^d
11	7	Me	52 ^d

^a Reaction conditions: 1.0 mmol aryl chloride, 2.0 mmol phenylmagnesium bromide, 2 mol% catalyst, 10 mL THF, room temperature.

^b GC yield, an average yield of two runs.

^c 32% of biphenyl was also obtained.

^d 26% of biphenyl was also obtained.

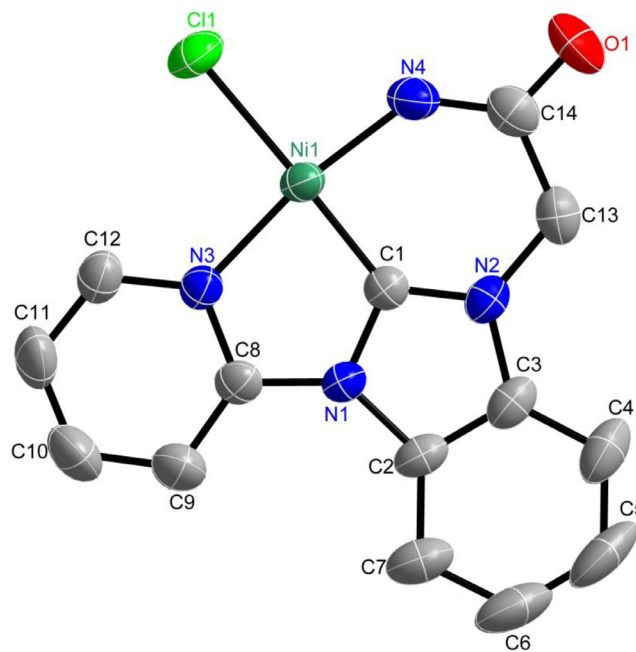


Fig. 5. Thermal ellipsoid plot of **6** at 50% probability level. Hydrogen atoms and solvent molecules are omitted for clarity. Selected bond lengths (\AA) and angles ($^{\circ}$): Ni-C(1), 1.790(3); Ni-N(4), 1.840(3); Ni-N(3), 1.932(3); Ni-Cl(1), 2.2117(10); N(4)-C(14), 1.325(4); C(1)-Ni-N(4), 89.27(14); C(1)-Ni-N(3), 81.81(13); N(4)-Ni-N(3), 170.72(12); C(1)-Ni-Cl(1), 177.73(11); N(4)-Ni-Cl(1), 91.93(10); N(3)-Ni-Cl(1), 96.91(8); N(2)-C(1)-N(1), 107.4(3).

rides ($\text{R}-\text{C}_6\text{H}_4\text{Cl}$, $\text{R} = \text{CN}$, Me, OMe) as substrates. Both complexes displayed very low activity in the reaction with 4-chlorobenzonitrile and only 5% yield was observed (entries 11 and 12). The low yield is caused by the cyano substituent of 4-chlorobenzonitrile, which induces a side reaction, therefore, reducing the formation of the desired coupling product. The yields were better with methoxy- and methyl-substituted chlorobenzene. Thus, 55 % of 4-methoxybiphenyl and 32% of biphenyl (entries 13 and 14), and 51% of 4-methylbiphenyl and 26% of biphenyl (entries 15 and 16), respectively, were obtained.

3. Conclusions

In summary, we have prepared several amido-functionalized NHC nickel carbene complexes, which include *cis* bis-bidentate complexes **3-5** and pincer-type complexes **6** and **7**. The preparation of complex **6** was unique, as acetate anion, a weak base, could deprotonate the C2-H and one of the amido protons. The chelating rings rendered the protons of the methylene moieties diastereotopic in complexes **3-5**, and the *cis* configurations resulted in steric hindrance, which prevents the free rotation of the ethyl and phenyl substituents in **4** and **5**, respectively, in solution. The catalytic activity of these nickel complexes was examined in Kumada cross-coupling reaction of phenylmagnesium bromide with aryl chlorides, in which complexes **6** and **7** displayed similar catalytic activities resulting in excellent to moderate yields.

4. Experimental

4.1. General procedures

THF was dried and freshly distilled prior to use. Other solvents and chemicals were of analytic reagent grade and used as received. Compounds $\text{NiCl}_2(\text{CH}_3\text{CN})_2$ [26], 1-acetamido-3-methylbenzimidazolium bromide [12a], 1-acetamido-3-ethylbenzimidazolium bromide [12b], 1-phenylbenzimidazole [13], and 1-(2-pyridyl)benzimidazole [14] were synthesized according to the literature methods. Elemental analyses were carried out on a Hitachi 270-30 spectrometer. ^1H NMR spectra (δ (TMS) = 0.00 ppm) were recorded on either a Bruker Avance DPX300 or a Bruker Avance II 400 spectrometer operating at 300.13 and 400.13 MHz, respectively. ^{13}C NMR spectra were recorded on the same spectrometers operating at 75.46 and 100.61 MHz, respectively. Infrared spectra were recorded on a Jasco FT/IR-460 Plus spectrometer with 4 cm^{-1} resolution. GC spectra were obtained with GC 9800 gas chromatograph equipped with a FID detector.

4.2. X-ray structure determination

Crystallographic data collections were carried out on a Nonius KappaCCD diffractometer with a graphite-monochromatored Mo $\text{K}\alpha$ radiation ($\lambda = 0.71073 \text{ \AA}$) at 150(2) or 296(2) K. Cell parameters were retrieved and refined using the DENZO-SMN [27] software on

all reflections. Data reduction was performed with the DENZO-SMN [27] software. Empirical absorption correction was based on the symmetry-equivalent reflections and was applied to the data using the SORTAV [28] program. Structural analysis was made using the SHELXTL program on a personal computer. The structure was solved using the SHELXS-97 [29] program and refined using the SHELXL-97 [30] program by a full-matrix least-squares method on F^2 values. All non-hydrogen atoms were refined anisotropically. Except for the amido hydrogens in **5**, which were found and refined isotropically, all the other hydrogen atoms were fixed at calculated positions and refined using a riding mode. Crystal data and structure refinement for the different compounds are given in supporting information. Crystal data, details of data collection and structure refinement for compounds **4-7** (CCDC 2014566-2014570) can be obtained from the Cambridge Crystallographic Data Centre via www.ccdc.cam.ac.uk/data_request/cif.

4.3. Preparations of complexes

4.3.1. Preparation of 1-acetamido-3-phenylbenzimidazolium bromide (**1**)

1-Phenylbenzimidazole (2.042 g, 10.5 mmol), 2-bromoacetamide (1.518 g, 11.0 mmol) and acetonitrile (25 mL) were placed into a 50 mL flask. The mixture was refluxed for 2 days followed by the solvent removal. The remaining solid was washed thrice with 20 mL portions of dichloromethane. The washed solid was dried resulting in 3.089 g of white powder (9.3 mmol, 89% yield). ^1H NMR (DMSO- d_6 , 400 MHz): δ 10.39 (s, 1H, NCHN), 8.15 (br s, 1H, NH₂), 8.09 (d, J = 8.0 Hz, 1H, C₆H₄), 7.86 (m, 3H, Ph, C₆H₄), 7.75 (m, 6H, Ph, C₆H₄, NH₂), 5.47 (s, 2H, CH₂). ^{13}C NMR (DMSO- d_6 , 100 MHz): δ 166.66 (C=O), 144.02 (NCN), 133.46, 132.25 (C=C), 131.15, 131.08, 130.99 (Ph), 127.94, 127.65 (C₆H₄), 125.56 (Ph), 114.66, 113.97 (C₆H₄), 49.29 (CH₂). IR (KBr): 3313(vw), 3294(vw), 3141(w), 2945(m), 2802(vw), 2742(vw), 2506(vw), 1838(vw), 1704(vs), 1693(s), 1566(w), 1561(w), 1406(w), 1385(s), 1306(vw), 1257(w), 1207(vw), 1081(vw), 1029(vw), 1020(vw), 862(vw), 781(w), 761(m), 694(vw), 669(vw), 662(vw), and 585(vw) cm⁻¹. Anal. Calc. For C₂₀H₂₂N₆O₃Ni: C, 53.01; H, 4.89; N, 18.55. Found: C, 52.93; H, 4.96; N, 18.44%.

4.3.2. Preparation of 1-acetamido-3-(2-pyridyl)benzimidazolium bromide (**2**)

A mixture of 1-(2-pyridyl)benzimidazole (3.123 g, 16.0 mmol) and 2-bromoacetamide (2.208 g, 16.0 mmol) in THF (25 mL) was refluxed for 2 days to form a white precipitate. The precipitate was isolated by filtration and washed with THF repeatedly. The resulting white solid was dried to result in 3.902 g of white powder (11.7 mmol, 73% yield). ^1H NMR (DMSO- d_6 , 400 MHz): δ 10.60 (s, 1H, NCHN), 8.78 (d, J = 4.8 Hz, 1H, py), 8.45 (m, 1H, py), 8.29 (td, J = 7.8 Hz, J =1.8 Hz, 1H, py), 8.07 (m, 3H, py+NH₂), 7.76 (m, 4H, C₆H₄+NH₂), 5.43 (s, 2H, CH₂). ^{13}C NMR (DMSO- d_6 , 100 MHz): δ 166.52 (C=O), 150.07 (py), 147.56 (NCN), 143.81, 141.20 (py), 132.63 (C=C), 129.64 (C=C), 128.18, 127.81 (C₆H₄), 125.79 (py), 117.62 (C₆H₄), 116.22 (py), 114.65 (C₆H₄), 49.42 (CH₂). IR (KBr): 3786(w), 3691(vw), 3349(s), 3172(vw), 2954(m), 2808(vw), 2687(vw), 2604(vw), 2382(vw), 2299(vw), 1684(vs), 1559(w), 1484(vw), 1463(vw), 1441(vw), 1399(w), 1355(vs), 1342(vw), 1334(vw), 1308(w), 1286(vw), 1261(m), 1218(w), 1180(vw), 1157(vw), 1132(vw), 1099(vw), 1051(w), 890(vw), 854(w), 827(vw), 786(m), 757(vw), 743(vw), 721(vw), 672(w), 573(vw), and 512(vw) cm⁻¹. Anal. Calc. For C₁₄H₁₃BrN₄O: C, 50.47; H, 3.93; N, 16.82. Found: C, 50.43; H, 4.00; N, 16.79%.

4.3.3. Preparation of [Ni(Me-bimy-CH₂CONH)₂] (**3**)

A 50 mL flask was charged with 1-acetamido-3-methylbenzimidazolium bromide (270.8 mg, 1.0 mmol),

NiCl₂(CH₃CN)₂ (105.8 mg, 0.5 mmol), K₂CO₃ (276.0 mg, 2.0 mmol), and MeOH (20 mL). The solution was refluxed for 1.5 h. The green solution changed color to yellow with formation of a yellow precipitate. After cooling, the solvent was removed, and the solid was washed with 100 mL of deionized water, then re-dissolved in methanol and filtered through a pad of Celite. The solvent was removed resulting in 180.0 mg of light yellow solid (0.41 mmol, 83% yield). Slow diffusion of ether into a solution of compound in methanol - chloroform afforded orange crystals suitable for X-ray diffraction analysis. Mp: 324-329°C. ^1H NMR (DMSO- d_6): δ 7.80 (d, J = 7.7 Hz, 1H, C₆H₄), 7.55 (d, J = 7.7 Hz, 1H, C₆H₄), 7.35 (m, 2H, C₆H₄), 5.19 (d, J = 16.3 Hz, 1H, CH₂), 4.75 (d, J = 16.3 Hz, 1H, CH₂), 4.49 (s, 1H, NH), 3.31 (s, 3H, CH₃). ^1H NMR (DMSO- d_6 , 120 °C): δ 7.70 (d, J = 6.7 Hz, 1H, C₆H₄), 7.52 (d, J = 7.5 Hz, 1H, C₆H₄), 7.36 (m, 2H, C₆H₄), 4.94 (br s, 2H, CH₂), 3.89 (br s, 1H, NH), 3.38 (s, 3H, CH₃). ^{13}C NMR (DMSO- d_6): δ 178.55 (NCN), 170.83 (C=O), 134.57, 133.85 (C=C), 123.94, 123.56, 111.37, 111.01 (C₆H₄), 50.64 (CH₂), 33.89 (CH₃). IR (KBr): 3330(vw), 3203(vw), 3059(vw), 3035(vw), 2941(vw), 2925(vw), 2865(vw), 1624(s), 1586(vs), 1460(w), 1433(vw), 1385(s), 1344(vw), 1312(w), 1257(vw), 1207(vw), 1174(vw), 1150(vw), 1130(vw), 1092(vw), 1026(vw), 1012(vw), 982(vw), 927(vw), 848(vw), 796(vw), 757(w), 733(vw), 689(vw), 584(vw), 571(vw), 558(vw) cm⁻¹. Anal. Calc. For C₂₀H₂₂N₆O₃Ni: C, 53.01; H, 4.89; N, 18.55. Found: C, 52.93; H, 4.96; N, 18.44%.

4.3.4. Preparation of [Ni(Et-bimy-CH₂CONH)₂] (**4**)

Complex **4** was prepared analogously to complex **3** from 1-acetamido-3-ethylbenzimidazolium bromide (284.2 mg, 1.0 mmol), NiCl₂(CH₃CN)₂ (106.0 mg, 0.5 mmol), K₂CO₃ (276.0 mg, 2.0 mmol), and MeOH (20 mL) as a light yellow solid (190.0 mg, 0.41 mmol, 82% yield). Slow diffusion of ether into a methanol solution of the compound afforded orange crystals suitable for X-ray diffraction analysis. Mp: 292-296°C. ^1H NMR (DMSO- d_6): δ 7.83 (d, J = 7.9 Hz, 1H, C₆H₄), 7.63 (d, J = 7.9 Hz, 1H, C₆H₄), 7.34 (m, 2H, C₆H₄), 5.09 (d, J = 16.4 Hz, 1H, CH₂(amide)), 4.78 (d, J = 16.4 Hz, 1H, CH₂(amide)), 4.52 (br s, 1H, NH), 4.31 (m, 1H, CH₂(ethyl)), 3.59 (m, 1H, CH₂(ethyl)), 1.19 (t, J = 7.1 Hz, 3H, CH₃). ^1H NMR (DMSO- d_6 , 180 °C): δ 7.68 (d, J = 7.9 Hz, 1H, C₆H₄), 7.54 (d, J = 7.9 Hz, 1H, C₆H₄), 7.36 (m, 2H, C₆H₄), 4.92 (s, 2H, CH₂(amide)), 4.00 (q, J = 5.6 Hz, 2H, CH₂(ethyl)), 3.72 (br s, 1H, NH), 1.36 (t, J = 7.1 Hz, 3H, CH₃). ^{13}C NMR (DMSO- d_6): δ 178.43 (NCN), 170.90 (C=O), 134.28, 133.57 (C=C), 123.99, 123.66, 111.31, 111.25 (C₆H₄), 50.79 (CH₂(amide)), 42.79 (CH₂(ethyl)), 15.35 (CH₃). IR (KBr): 3340(vw), 3246(vw), 3065(vw), 3034(vw), 2988(vw), 2965(vw), 2931(vw), 2867(vw), 1618(s), 1589(vs), 1476(vw), 1449(w), 1396(m), 1385(m), 1336(vw), 1305(w), 1270(vw), 1237(vw), 1207(vw), 1191(vw), 1169(vw), 1111(vw), 1081(vw), 1034(vw), 1012(vw), 979(vw), 930(vw), 881(vw), 845(vw), 818(vw), 776(vw), 758(w), 745(w), 719(vw), 612(vw) cm⁻¹. Anal. Calc. for C₂₂H₂₅N₆O_{2.5}Ni: C, 55.96; H, 5.34; N, 17.80. Found: C, 55.90; H, 5.18; N, 17.85%.

4.3.5. Preparation of [Ni(Ph-bimy-CH₂CONH)₂] (**5**)

A 50 mL flask was charged with 1-acetamido-3-phenylbenzimidazolium bromide (332.2 mg, 1.0 mmol), Ni(OAc)₂ (88.2 mg, 0.5 mmol), and TBAB (1.0 g). The solution was heated to 130 °C for 3 h. The solid dissolved yielding a green solution. The solution was cooled to room temperature and an orange precipitate was formed. The resulting solid was washed with 100 mL of deionized water, and then dissolved in methanol and filtered through a pad of Celite. After the solvent was removed, 90.2 mg of light yellow solid (0.16 mmol, 32% yield) was obtained. Crystals suitable for X-ray diffraction analysis were isolated from methanol solution. Mp: 303-306°C. ^1H NMR (DMSO- d_6): δ 7.88 (br s, 2H, Ph), 7.50 (d, J = 8.0 Hz, 1H, C₆H₄), 7.36 (br s, 2H, Ph), 7.26 (t, J = 7.1 Hz, 1H, C₆H₄), 7.19 (m, 3H, Ph+C₆H₄), 4.62 (br

s, 1H, NH), 4.50 (d, $J = 16.2$ Hz, 1H, CH₂), 4.42 (d, $J = 16.2$ Hz, 1H, CH₂). ¹H NMR (DMSO-d₆, 100 °C): δ 7.86 (d, $J = 7.6$ Hz, 2H, Ph), 7.44 (d, $J = 8.0$ Hz, 1H, C₆H₄), 7.37 (t, $J = 7.6$ Hz, 2H, Ph), 7.28 (t, $J = 7.5$ Hz, 1H, C₆H₄), 7.22 (t, $J = 7.2$ Hz, 2H, Ph+C₆H₄), 7.17 (d, $J = 7.9$ Hz, 1H, C₆H₄), 4.46 (s, 2H, CH₂), 4.16 (br s, 1H, NH). ¹³C NMR(DMSO-d₆): δ 180.15 (NCN), 170.34 (C=O), 137.26 (Ph), 133.50, 133.27 (C=C), 129.41, 128.70, 126.23 (Ph), 124.24, 123.96, 110.78, 110.61 (C₆H₄), 50.23 (CH₂). IR (KBr): 3332(vw), 3200(vw), 3095(vw), 3067(vw), 3036(vw), 2971(vw), 2925(vw), 2888(vw), 1621(vs), 1591(vs), 1501(vw), 1473(w), 1457(vw), 1416(w), 1385(s), 1303(m), 1284(w), 1243(vw), 1215(w), 1191(vw), 1158(vw), 1092(w), 1070(w), 1048(w), 1018(w), 911(vw), 889(vw), 842(vw), 812(vw), 785(vw), 755(m), 748(m), 697(m), 626(vw), 606(vw), 497(vw) cm⁻¹. Anal. Calc. for C₃₀H₂₈N₆O₄Ni: C, 60.53; H, 4.74; N, 14.12. Found: C, 60.44; H, 4.80; N, 14.05%.

4.3.6. Preparation of [Ni(Py-bimy-CH₂CONH)Cl] (6)

1-Acetamido-3-(2-pyridyl)benzimidazolium bromide (333.2 mg, 1.0 mmol), NiCl₂(CH₃CN)₂ (211.4 mg, 1.0 mmol), NaOAc (164.4 mg, 2.0 mmol), and 20 mL of MeOH - DMF (1:3, v/v) were placed into a 50 mL flask. The mixture was refluxed at 120 °C for 24 h yielding a yellow-brown precipitate. The solvents were removed, and the resulting solid was washed with methanol several times. After methanol was removed, 300.0 mg of yellow solid (0.87 mmol, 87% yield) was isolated. Crystals suitable for X-ray diffraction analysis were obtained from DMSO - ether - ethyl acetate. Mp: 309–311°C. ¹H NMR (DMSO-d₆): δ 8.84 (br s, 1H, py), 8.36 (d, $J = 7.7$ Hz, 1H, C₆H₄), 8.29 (m, 2H, py), 7.83 (d, $J = 7.4$ Hz, 1H, C₆H₄), 7.58 (m, 2H, C₆H₄), 7.52 (t, $J = 6.4$ Hz, 1H, py), 4.84 (s, 2H, CH₂), 3.73 (br s, 1H, NH). IR (KBr): 3333(vw), 3121(vw), 3101(vw), 3068(vw), 2965(vw), 2930(vw), 1596(vs), 1533(vw), 1482(s), 1477(s), 1427(vw), 1385(m), 1366(w), 1269(vw), 1259(vw), 1241(vw), 1203(vw), 1095(vw), 1023(vw), 1012(vw), 908(vw), 856(vw), 766(w), 740(w), 732(vw), 617(vw) cm⁻¹. Anal. Calc. for C₁₄H₁₁CIN₄ONi: C, 48.68; H, 3.21; N, 16.22. Found: C, 48.60; H, 3.03; N, 15.90%.

4.3.7. Preparation of [Ni(Py-bimy-CH₂CONH)Br] (7)

1-Acetamido-3-(2-pyridyl)benzimidazolium bromide (333.3 mg, 1.0 mmol), Ni(OAc)₂ (176.1 mg, 1.0 mmol), and TBAB (1.0 g) were placed into a 50 mL flask. The solution was heated to 130 °C for 3 h. The solid dissolved yielding a yellow solution. The solution was cooled to room temperature and an orange precipitate was formed. The resulting solid was washed with 50 mL of methanol and then dried, resulting in 257.2 mg orange solid (0.66 mmol, 66% yield). Crystals suitable for X-ray diffraction analysis were obtained from DMSO - ether - acetone. Mp: 342–344°C. ¹H NMR (DMSO-d₆): δ 8.61 (d, $J = 5.7$ Hz, 1H, py), 8.34 (m, 3H, py+C₆H₄), 7.84 (d, $J = 7.1$ Hz, 1H, C₆H₄), 7.56 (m, 2H, C₆H₄), 7.52 (t, $J = 6.3$ Hz, 1H, py), 4.88 (s, 2H, CH₂), 4.15 (br s, 1H, NH). IR (KBr): 3323(vw), 3117(vw), 3100(vw), 3082(vw), 3070(vw), 3031(vw), 2962(vw), 2927(vw), 2851(vw), 1598(vs), 1536(vw), 1508(vw), 1482(m), 1424(vw), 1383(vw), 1366(w), 1340(vw), 1303(vw), 1259(w), 1240(vw), 1201(vw), 1143(vw), 1098(w), 1055(w), 1021(w), 914(vw), 862(vw), 803(w), 763(w), 745(w), 711(vw), 620(vw), 587(vw) cm⁻¹. Anal. Calc. for C₁₄H₁₁BrN₄ONi: C, 43.13; H, 2.84; N, 14.37. Found: C, 43.19; H, 2.90; N, 14.35%.

4.3.8. General procedure for Kumada coupling catalyzed by complexes 3–7

In a typical run, a two-neck flask was charged with 0.02 mole of a nickel(II) complex and 10 mL of anhydrous THF under nitrogen atmosphere. Aryl chloride (1.0 mmol) and phenylmagnesium bromide (2.0 mmol) were added subsequently. Upon the addition of these reagents, the solution changed color to orange-brown. The mixture was stirred at room temperature for 6 h. Water was

added to the reaction mixture, followed by extraction with ether (3×20 mL). The organic fractions were combined and dried with anhydrous magnesium sulfate. After the volatiles were removed in *vacuo*, a light brown solid was isolated. The product yield was calculated by integration the area of peaks in a gas chromatogram.

Declaration of Competing Interest

The authors declare that they have no known competing financial interests or personal relationships that could have appeared to influence the work reported in this paper.

Acknowledgments

This work was supported by the Ministry of Science and Technology of the ROC through Grant MOST 108-2113-M-259-003.

Supplementary materials

Supplementary material associated with this article can be found, in the online version, at doi:10.1016/j.jorgchem.2020.121543.

References

- [1] A.J. Arduengo III, R.L. Harlow, M. Kline, J. Am. Chem. Soc. 113 (1991) 361–363.
- [2] (a) D.J. Nelson, S.P. Nolan, N-Heterocyclic Carbenes: Effective Tools for Organometallic Synthesis, Wiley-VCH, Weinheim, Germany, 2014; (b) D.J. Nelson, S.P. Nolan, 2013 Chem. Soc. Rev., 42 6723–6753.
- [3] (a) V. Dragutan, I. Dragutan, L. Delaude, A. Demonceau, Coord. Chem. Rev. 251 (2007) 765–794; (b) F.E. Hahn, M.C. Jahnke, Angew. Chem. Int. Ed. 47 (2008) 3122–3172; (c) S.P. Nolan, Acc. Chem. Res. 44 (2011) 91–100; (d) F. Lazreg, F. Nahra, C.S.J. Cazin, Coord. Chem. Rev. 293–294 (2015) 48–79; (e) A. Nasr, A. Winkler, M. Tamm, Coord. Chem. Rev. 316 (2016) 68–124.
- [4] (a) A. de Meijere, F. Diederich, Metal-Catalyzed Cross-Coupling Reactions, Wiley-VCH, Weinheim, 2004; (b) S. Würtz, F. Glorius, 2008 Acc. Chem. Res., 41 1523–1533; (c) R. Zhong, A.C. Lindhorst, F.J. Groche, F.E. Kühn, 2017 Chem. Rev., 117 1970–2058; (d) O. Schuster, L. Yang, H.G. Raubenheimer, M. Albrecht, 2009 Chem. Rev., 109 3445–3478; (e) N. Marion, S.P. Nolan, 2008 Acc. Chem. Res., 41 1440–1449; (f) G.C. Fortman, S.P. Nolan, 2011 Chem. Soc. Rev., 40 5151–5169; (g) E.A.B. Kantchev, C.J. O'Brien, M.G. Organ, 2007 Angew. Chem. Int. Ed., 46 2768–2813.
- [5] (a) A.A. Danopoulos, T. Simler, P. Braunstein, Chem. Rev. 119 (2019) 3730–3961; (b) M. Henrion, V. Ritleng, M. Chetcuti, ACS Catal. 5 (2015) 1283–1302.
- [6] (a) J. Duczynski, A.N. Sobolev, S.A. Moggach, R. Dorta, S.G. Stewart, Organometallics 39 (2020) 105–115; (b) J.C. Bernhammer, H.V. Huynh, Organometallics 33 (2014) 5845–5851; (c) S. Gu, J. Du, J. Huang, Y. Guo, L. Yang, W. Xu, W. Chen, Dalton Trans 46 (2017) 586–594; (d) A. Ohtsuki, K. Yanagisawa, T. Furukawa, M. Tobisu, N. Chatani, J. Org. Chem. 81 (2016) 9409–9414; (e) P.-A. Payard, L.A. Pereo, I. Ciolfini, L. Grimaud, ACS Catal. 8 (2018) 4812–4823.
- [7] (a) R. Jothibasu, K.-W. Huang, H.V. Huynh, Organometallics 29 (2010) 3746–3752; (b) I.A. Bhat, I. Avinash, G. Anantharaman, Organometallics 38 (2019) 1699–1708; (c) Ł. Banach, P.A. Guńska, W. Buchowicz, Dalton Trans 45 (2016) 8688–8692; (d) S. Gu, W. Chen, Organometallics 28 (2009) 909–914.
- [8] (a) J. Xia, Y. Zhang, J. Zhang, Z. Jian, Organometallics 38 (2019) 1118–1126; (b) W. Li, H. Sun, M. Chen, Z. Wang, D. Hu, Q. Shen, Y. Zhang, Organometallics 24 (2005) 5925–5928.
- [9] (a) Q. Zhao, G. Meng, S.P. Nolan, M. Szostak, Chem. Rev. 120 (2020) 1981–2048; (b) M. Henrion, B.P. de Cardoso, V. César, M.J. Chetcuti, V. Ritleng, Organometallics 36 (2017) 1113–1121; (c) M.R. Elsby, J. Liu, S. Zhu, L. Hu, G. Huang, S.A. Johnson, Organometallics 38 (2019) 436–450; (d) W.-B. Zhang, X.-T. Yang, J.-B. Ma, Z.-M. Su, S.-L. Shi, J. Am. Chem. Soc. 141 (2019) 5628–5634.
- [10] (a) V.S. Thoi, N. Kornienko, C.G. Margarit, P. Yang, C.J. Chang, J. Am. Chem. Soc. 135 (2013) 14413–14424; (b) Z. Lu, T.J. Williams, ACS Catal 6 (2016) 6670–6673.
- [11] (a) D. Pugh, A.A. Danopoulos, Coord. Chem. Rev. 251 (2007) 610–641; (b) E. Peris, R.H. Crabtree, Coord. Chem. Rev. 248 (2004) 2239–2246.
- [12] (a) S.-C. Chen, H.-H. Hsueh, C.-H. Chen, C.-S. Lee, F.-C. Liu, I.J.B. Li2n, G.-H. Lee, S.-M. Peng, Inorg. Chim. Acta 362 (2009) 3343–3350; (b) Y.-C. Lin, H.-H. Hsueh, S. Kanne, L.-K. Chang, F.-C. Liu, I.J.B. Lin, G.-H. Lee, S.-M. Peng, Organometallics 32 (2013) 3859–3869; (c) K.M. Lee, J.C.C. Chen, C.J. Huang, I.J.B. Lin, CrystEngComm 9 (2007) 278–281.
- [13] L. Zhu, L. Cheng, Y. Zhang, R. Xie, J. You, J. Org. Chem. 72 (2007) 2737–2743.
- [14] B. Pilarski, Liebigs Ann. Chem. (1983) 1078–1080.
- [15] G. Meng, L. Kalakis, S.P. Nolan, M. Szostak, Tetrahedron Lett 60 (2019) 378–381.
- [16] (a) H.W. Wanzlick, H.J. Schonherr, Angew. Chem. Int. Ed. 7 (1968) 141–142; (b) H.V. Huynh, C. Holtgrewe, T. Pape, L.L. Koh, E. Hahn, Organometallics 25 (2006) 245–249.

- [17] (a) J. Berding, T.F. van Dijkman, M. Lutz, A.L. Spek, E. Bouwman, Dalton Trans (2009) 6948–6955; (b) C.-Y. Liao, K.-T. Chan, Y.-C. Chang, C.-Y. Chen, C.-Y. Tu, C.-H. Hu, H.M. Lee, Organometallics 26 (2007) 5826–5833; (c) S. Kumar, A. Narayanan, M.N. Rao, M.M. Shaikh, P. Ghosh, J. Organomet. Chem. 696 (2012) 4159–4165; (d) L. Ray, M.M. Shaikh, P. Ghosh, P. Eur, J. Inorg. Chem. (2009) 1932–1941; (e) C.-Y. Liao, K.-T. Chan, J.-Y. Zeng, C.-H. Hu, C.-Y. Tu, H.M. Lee, Organometallics 26 (2007) 1692–1702; (f) F. Jean-Baptiste-dit-Dominique, H. Gornitzka, C. Hemmert, Organometallics 29 (2010) 2868–2873.
- [18] (a) P.L. Chiu, C.-L. Lai, C.-F. Chang, C.-H. Hu, H.M. Lee, Organometallics 24 (2005) 6169–6178; (b) C.-C. Lee, W.-C. Ke, K.-T. Chan, C.-L. Lai, C.-H. Hu, H.M. Lee, Chem-Eur. J. 13 (2007) 582–591; (c) X. Wang, S. Liu, G.-X. Jin, Organometallics 23 (2004) 6002–6007; (d) M.V. Baker, B.W. Skelton, A.H. White, C.C. Williams, J. Chem. Soc. Dalton Trans. (2001) 111–120; (e) W.N.O. Wylie, A.J. Lough, R.H. Morris, Organometallics 28 (2009) 6755–6761; (f) Y. Kong, M. Cheng, H. Ren, S. Xu, H. Song, M. Yang, B. Liu, B. Wang, Organometallics 28 (2009) 5934–5940; (g) I.A. Bhat, I. Avinash, G. Anantharaman, Organometallics 38 (2019) 1699–1708.
- [19] L. Pauling, in: The Nature of The Chemical Bond, vol. 256, third ed., Cornell University Press, Ithaca, NY, 1960, pp. 224–225.
- [20] L. Pauling, in: The nature of the Chemical Bond, 3rd. ed., Cornell University Press, Ithaca, NY, 1960, pp. 224–228, 256–258.
- [21] (a) A.G. Nair, R.T. McBurney, M.R.D. Gatus, D.B. Walker, M. Bhadhave, B.A. Messerle, J. Organomet. Chem. 845 (2017) 63–70; (b) C. Chen, H. Qiu, W. Chen, J. Organomet. Chem. 696 (2012) 4166–4172; (c) C. Zhang, Z.-X. Wang, Organometallics 28 (2009) 6507–6514.
- [22] (a) J.W. Nugent, G.E. Martinez, D.L. Gray, A.R. Fout, Organometallics 36 (2017) 2987–2995; (b) K. Zhang, M. Conda-Sheridan, S.R. Cooke, J. Louie, Organometallics 30 (2011) 2546–2552; (c) Y.-P. Huang, C.-C. Tsai, W.-C. Shih, Y.-C. Chang, S.-T. Lin, G.P.A. Yap, I. Chao, T.-G. Ong, Organometallics 28 (2009) 4316–4321.
- [23] (a) K. Tamao, K. Sumitani, M. Kumada, J. Am. Chem. Soc. 94 (1972) 4374–4376; (b) A.H. Cherney, N.T. Kadunce, S.E. Reisman, Chem. Rev. 115 (2015) 9587–9652; (c) S. Lou, G.C. Fu, J. Am. Chem. Soc. 132 (2010) 1264–1266; (d) Z.-X. Wang, N. Liu, Eur. J. Inorg. Chem. 2012 (2012) 901–911.
- [24] V.P.W. Böehm, C.W.K. Gstöttmayr, T. Weskamp, W.A. Herrmann, Angew. Chem. Int. Ed. 40 (2001) 3387–3389.
- [25] (a) G. van Koten, D. Milstein, Topics in Organometallic Chemistry, Organometallic Pincer Chemistry, Vol. 40, Springer, 2013; (b) R.E. Andrew, L. González-Sebastián, A.B. Chaplin, 2016 Dalton Trans, 45 1299–1305; (c) M.H.P. Rietveld, D.M. Grove, G. van Koten, 1997 New J. Chem., 21 751–771; (d) N. Selander, K.J. Szabó, 2011 Chem. Rev., 111 2048–2076.
- [26] B.J. Hathaway, D.G. Holah, J. Chem. Soc. (1964) 2400–2448.
- [27] Z. Otwinowsky, W. Minor, DENZO-SMN, Methods Enzymol. 276 (1997) 307–326.
- [28] (a) Acta Crystallogr. A51 (1995) 33–38; (b) R.H. Blessing, J. Appl. Crystallogr. 30 (1997) 421–426.
- [29] G.M. Sheldrick, SHELXS-97, Acta Crystallogr. A46 (1990) 467–473.
- [30] G.M. Sheldrick, SHELXL-97, University of Göttingen, Göttingen, Germany, 1997.